Electronic Supplementary Material (ESI) for Materials Advances.


Supplemental Information for:

# Thermomorphological and Mechanical Properties of Vulcanized Octenyl Succinate/Terpenoid-Derivatized Corn Starch Composites

Moira K. Lauer, Andrew G. Tennyson* and Rhett C. Smith*

## Instrumentation

Fourier transform infrared spectra were obtained using an IR instrument (Shimadzu IRAffinity-1S) with an ATR attachment. Scans were collected over the range 400–4000 $cm^{-1}$ at ambient temperature with a resolution of 8. TGA was recorded (Mettler Toledo TGA 2 STARe System) over the range 20–800 °C with a heating rate of 10 °C·$min^{-1}$ under a flow of $N_2$ (100 mL·$min^{-1}$). Each measurement was acquired in duplicate and presented results represent an average value. DSC was acquired (Mettler Toledo DSC 3 STARe System) over the range −60 to 150 °C with a heating rate of 5 °C·$min^{-1}$ under a flow of $N_2$ (200 mL·$min^{-1}$). Each DSC measurement was carried out over five heat-cool cycles. Each measurement was acquired in duplicate to ensure consistent results were obtained. Carbon disulfide extractions were performed by suspending 0.3 g of finely ground material (measured to 0.0001 g) in 20 mL of $CS_2$, allowing the solid to settle for 30 minutes, pipetting off the supernatant into a separate vial, and adding another 20 mL of $CS_2$. This process was repeated an additional 3 times so that a total of 5 washes was performed. The residual $CS_2$ was evaporated under a flow of $N_2$ and each vial was weighed to determine the fraction that was soluble (collected as supernatant) or insoluble (remained in the initial vial). DMA was performed (Mettler Toledo DMA 1 STARe System) in single cantilever mode. DMA samples were cast from silicone resin molds (Smooth-On Oomoo® 30 tin-cure). Samples were manually sanded to ensure uniform dimensions. The sample dimensions were approximately 15 x 8 x 1.5 mm. Sample dimensions were measured with a digital calliper with ±0.01 mm resolution. Samples were clamped by hand tightening due to their brittleness. The force was varied from 0 to 10 N with a ramp rate of 0.2 N·$min^{-1}$ measured isothermally at 25 °C. Compressional analysis was performed on a Mark-10 ES30 test stand equipped with a M3-200 force gauge (1 kN maximum force with ±1 N resolution). Compression cylinders were cast from silicone resin molds (Smooth-On Oomoo® 30 tin-cure) with diameters of approximately 6 mm and heights of approximately 10 mm. Samples were manually sanded to ensure uniform dimensions and measured with a digital calliper with ±0.01 mm resolution. Compressional analysis was performed in triplicate and results were averaged.

Synthesis of Starch Derivatives.

The synthesis and characterization of oxidized starch (**OS**) with a degree of substitution of 0.0263 was previously reported.[1]

Esterification of **OS** was prepared based on a previously reported procedure.[2]

Briefly, into a 100 mL round bottom flask equipped with a Teflon-coated stir bar was placed **OS** (15.112 g, 90.1 mmol), leucine (0.760 g, 5.79 mmol), and enough geraniol (28.376 g, 184 mmol) to completely submerge the solid material. The flask was sealed with a rubber septum and placed in a thermostat-controlled oil bath set to 80 °C. The reaction was allowed to continue for 4 days. The material was allowed to cool, filtered, and washed with ethanol (3 x 50 mL). The material was dried for 3 days in a vacuum oven (40 °C, 70 cmHg), frequently releasing and reapplying the vacuum. The reaction yield was quantitative. The material was sieved using an ASTM 50 sieve (300 μm particle size cut-off).

Synthesis of **GSSx** materials

The moisture content (~10%) of **GES** was taken into consideration when preparing 90 and 95 wt% sulfur materials. Reaction conditions were assessed for **$GSS_{90}$** and then applied for **$GSS_{95}$**. Because of necessarily long reaction times, reactions were conducted under nitrogen. The appropriate amount of sulfur and **GES** were combined in a 20 mL glass vial equipped with a Teflon coated stir bar. The reactions were sealed with a septum held down by copper wire. Reaction vials were purged with nitrogen for 15 minutes and placed in a thermostat-controlled oil bath set to 180 °C. Periodically, the reactions were removed from the oil bath, allowed to cool, manually scraped down with a metal spatula, resealed, purged with nitrogen for 15 minutes, and placed back in the oil bath. A total of 8 heating cycles was performed totaling 15 hours. Reactions were stopped at t=1 h, t=2 h, t=4 h, t=6h, t=8 h, t=10 h, t=12 h, and t=15 h. This process was necessary due to the incompatibility of the organic fraction with sulfur which would largely precipitate out and adhere to the sides of the vial above the surface of the reaction mixture. Over the 15 hour process, homogenization was possible.

**$OSS_{90}$** was prepared from sulfur (9.002 g) and **GES** (1.108 g).

Elemental analysis: S: 88.10%; C: 5.34%, H: 0.70%

**$OSS_{95}$** was prepared from sulfur (9.491 g) and **GES** (0.555 g).

Elemental analysis: S: 92.36%; C: 2.65%; H: 0.24%

PXRD data for starch, **OS**, and **GES**[3]

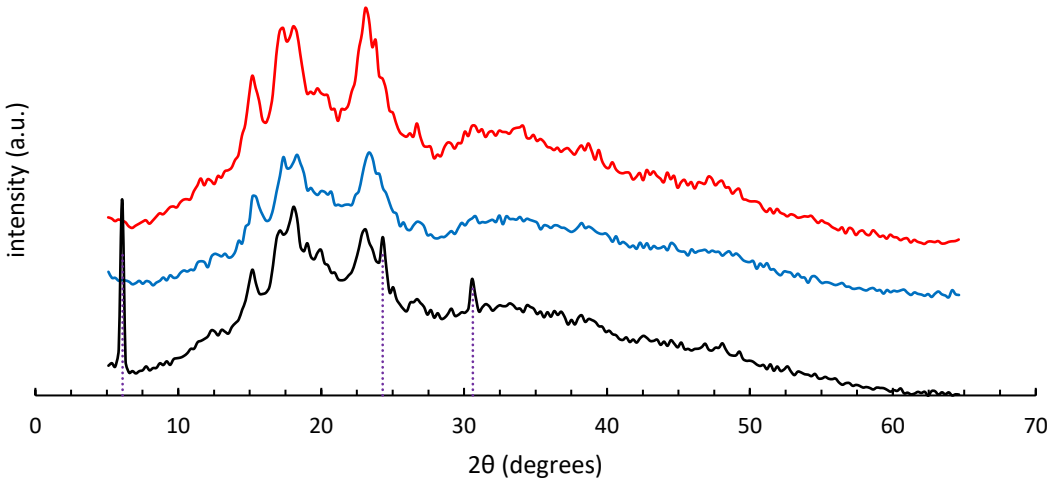


**Figure S1.** Stacked PXRD patterns of unmodified corn starch (red), **OS** (blue), and **GES** (black). The three additional peaks seen in **GES** (denoted by purple dotted lines at 6.15, 24.55, and 30.61 degrees) are attributed to leucine impurities. These impurities could not be visualized by $^{1}$H NMR indicating the impurity is relatively small. These peaks were excluded in calculating the percent crystallinity. Values for crystallinity were found to be 20.9, 15.8, and 20.2% for starch, **OS**, and **GES**, respectively indicating some of the amorphous regions were solubilized in geraniol during reaction or in ethanol during workup.

FTIR data of **OS** and **GES**

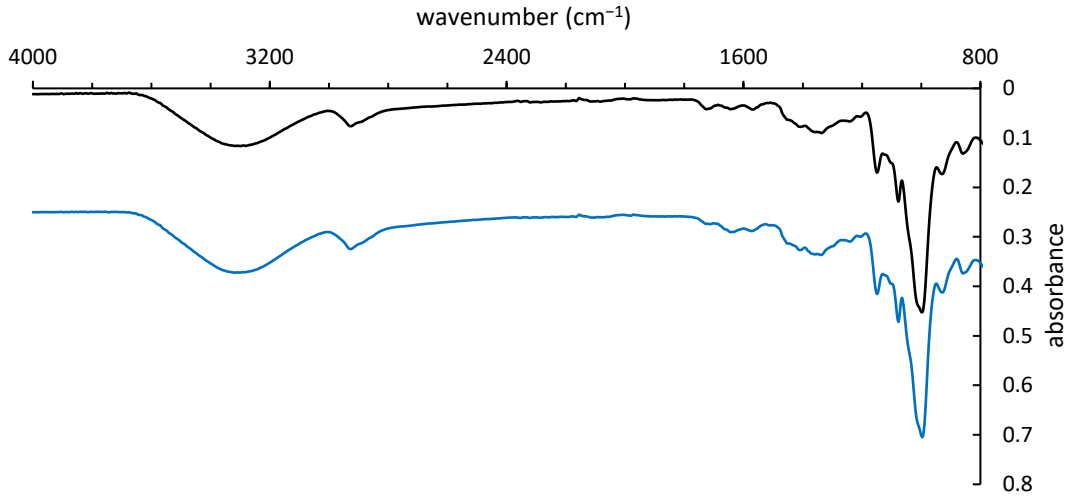


**Figure S2.** ATR-FTIR data for **OS** (black) and **GES** (blue) showing nearly indistinguishable features. The intensity was normalized at 999 $cm^{-1}$ and were offset by 0.25 absorbance units for clarity.

Proton NMR data for **OS**, **GES**, and geraniol

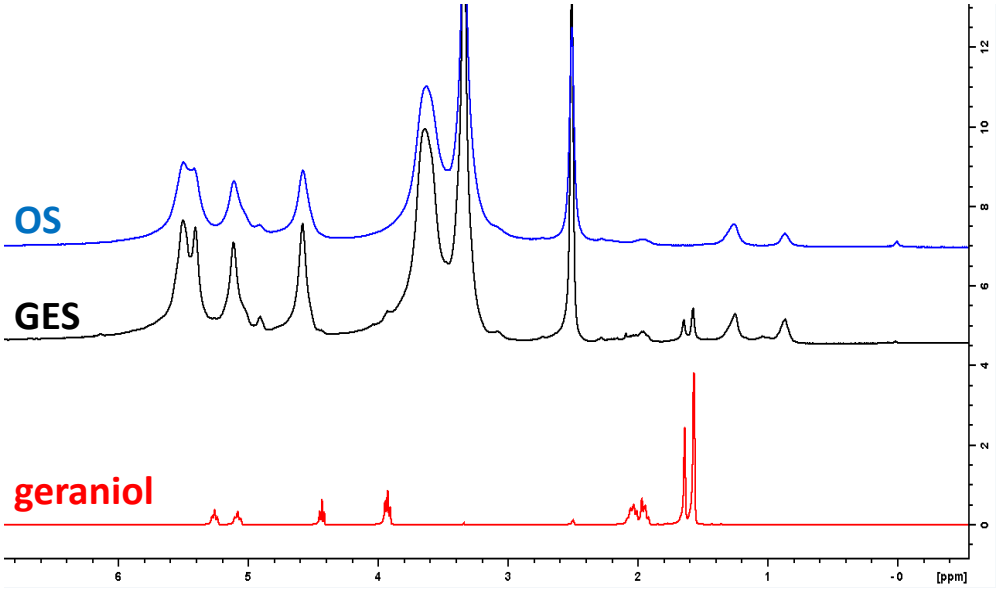


**Figure S3.** Proton NMR spectra of **OS** (blue), **GES** (black), and geraniol (red) in DMSO at room temperature. All spectra were calibrated to the peak for the solvent peak. Starch samples were largely solubilized by sonicating at 70 °C for 2 hours and storing overnight at room temperature over molecular sieves. Successful modification can be observed by the appearance of new peaks in **GES** due to functionalization with geraniol.

TGA of starch, **OS**, and **GES**

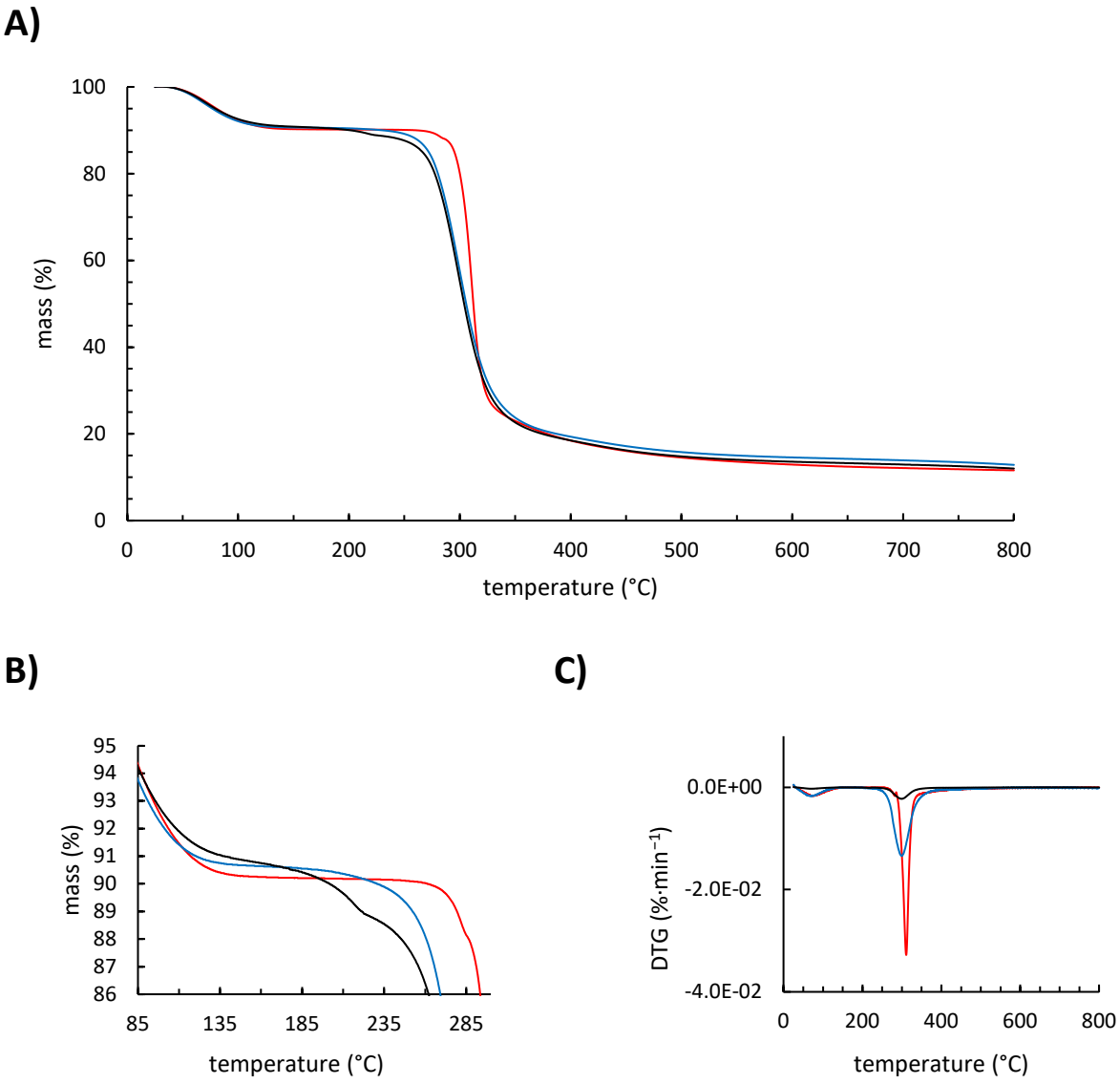


**Figure S4.** Mass loss curves for starch (red), **OS** (blue), and **GES** (black) over the range 25–800 °C (A), over the range 85–300 °C (B), and the corresponding DTG curves (C). With successive modification of starch, decomposition occurs over a broader temperature range and water is desorbed more slowly. The char yields for starch, **OS**, and **GES** were found to be 10.7, 11.6, 11.9%, respectively

Degree of esterification determination of **GES**

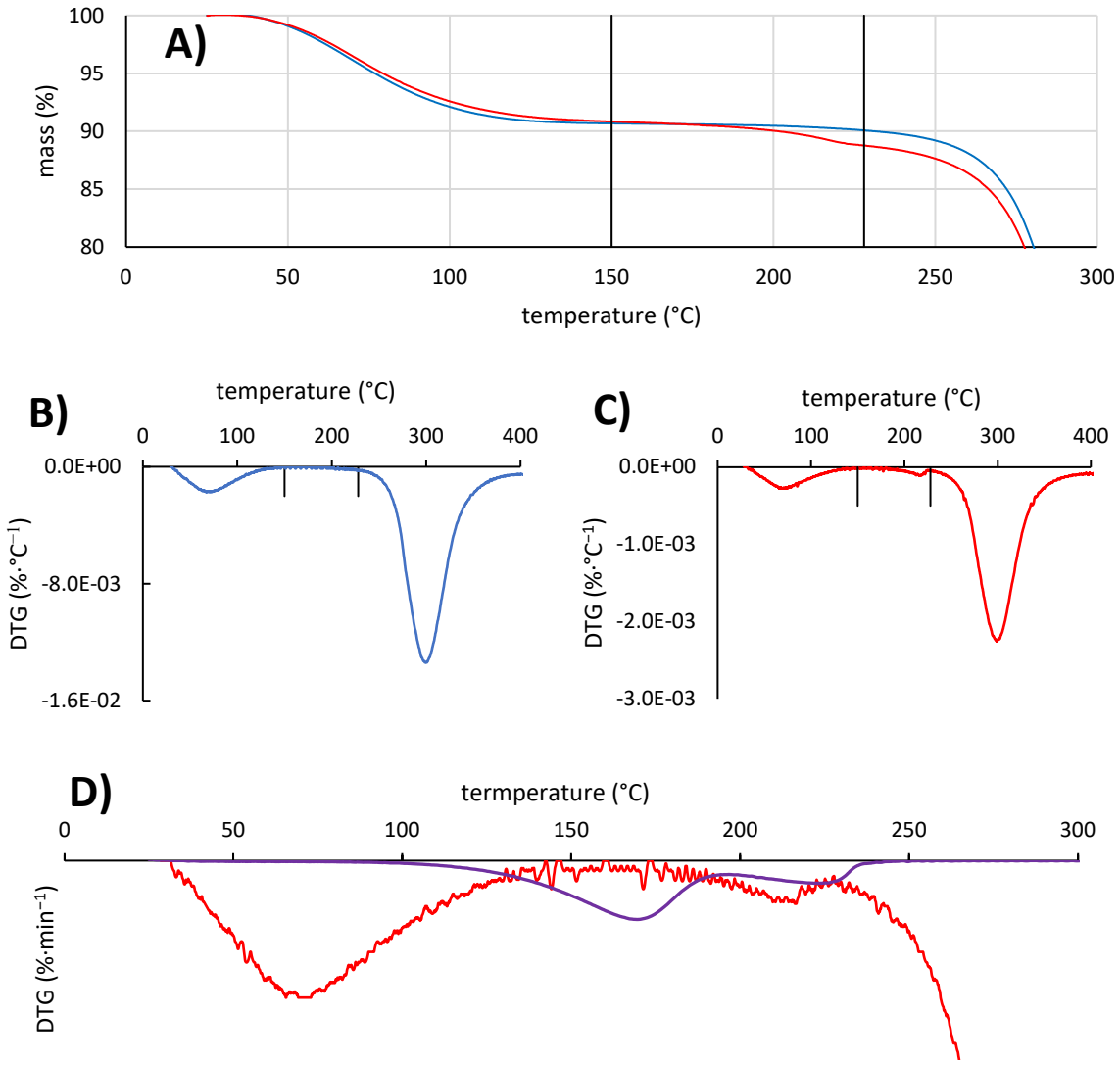


**Figure S5.** TGA data used to determine the degree of substitution of **GES**. Panel A shows the mass loss curves for **OS** (blue) and **GES** (red) over the range 25–300 °C with horizontal black lines showing the range of data attributable to decomposition of pendant geraniol chains (150–228 °C). Panels B and C show the DTG curves for **OS** (blue) and **GES** (red), respectively. Panel D shows the DTG curves for **GES** (red) and geraniol (purple) where the intensity has been normalized to more clearly show how the curves line up. The two-step mass loss observed for geraniol is believed to be evaporation followed by decomposition. In **GES**, covalent binding of geraniol to the starch prevents volatilization.

Cont'd

**Table S1.** TGA data used for the calculation of **GES** degree of substitution

| | **OS** | | | **GES** | | |
|---|---|---|---|---|---|---|
| | average[a] | std. dev.[b] | % error | average[a] | std. dev.[b] | % error |
| mass at 150 °C | 90.00 | 0.86 | | 90.47 | 0.41 | |
| mass at 228 °C | 89.44 | 0.72 | | 88.46 | 0.48 | |
| mass difference | **0.56** | 0.16 | 28% | **2.02** | 0.11 | 5.5% |

[a]Average of quadruplicate runs. [b]Standard deviation of quadruplicate runs. [c]The mass loss observed between 150 and 228 °C.

All samples used for analysis were ran in quadruplicate to ensure consistent results and minimum standard deviation. The largest error was introduced by the variability in mass loss of **OS** between 150 and 228 °C. Taking this variability into consideration provided degree of substitution accuracy of <0.2%. In the following equation $\Delta_{\%}$ is the difference in mass loss observed between 150 and 228 °C for **OS** and **GES**, $M_{ger}$ and $M_{GES}$ are the molecular weights of geraniol and GES, respectively, and $m_{OS@228}$ is the residual mass at 228 °C for **OS**.

**Equation S1:**

$$DS = \frac{\Delta_{\%} * M_{ger}}{m_{\boldsymbol{OS}@228} * M_{\boldsymbol{GES}}} = \frac{(2.02 - 0.56) * 154.25}{88.46 * 167.67} = 1.5\%$$

DSC data for starch, **OS**, and **GES**

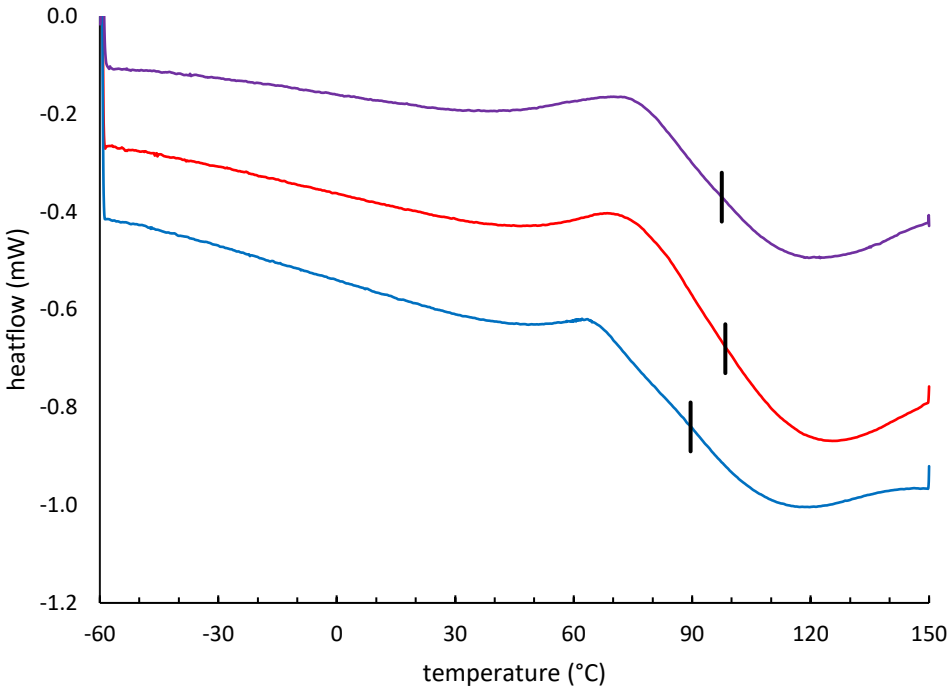


**Figure S6.** DSC third heating curves for starch (red), **OS** (blue), and **GES** (purple). The $T_g$ values are denoted with a black vertical line for each sample. Curves were found to be quite similar and correlate well with the calculated crystallinities from PXRD where higher $T_g$ values are observed for more crystalline materials.

**Table S2.** DSC $T_g$ values and correlating percent crystallinities

| material | $T_g$ | % xtl[a] |
|---|---|---|
| starch | 98.4 | 20.9 |
| **OS** | 89.6 | 15.8 |
| **GES** | 97.5 | 20.2 |

[a]Calculated from PXRD data.

TGA for **GSS$_x$** materials

**A)**

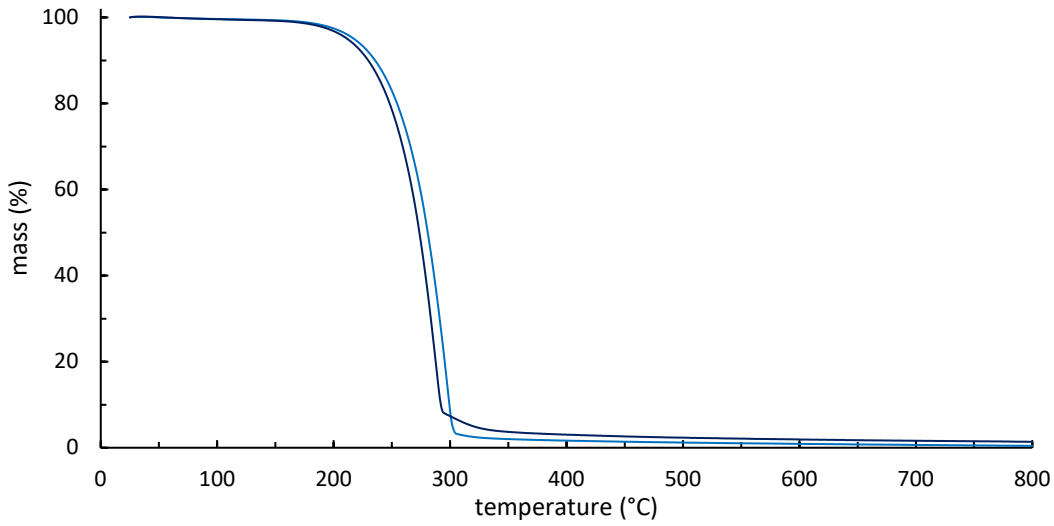


**B)**

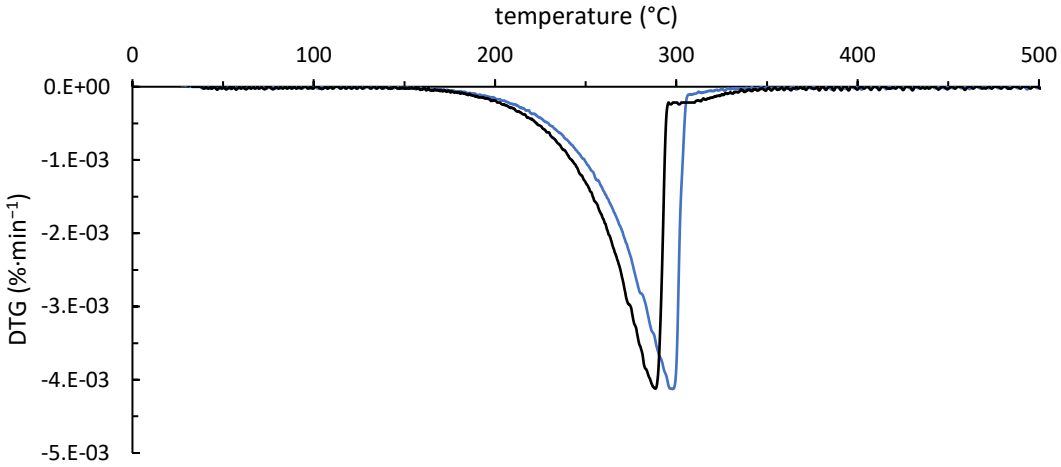


**Figure S7.** Mass loss curves over the range 25–800 °C for **GSS$_{95}$** (blue) and **GSS$_{90}$** (black) (A) and the corresponding DTG curves over the range 25–500 °C (B). Onset of sulfur sublimation (the primary mass loss feature) occurs at a slightly lower temperature for **GSS$_{90}$** due to a more significant disruption of the crystal structure. A small second mass loss feature is observed in both curves due to the decomposition of the organic portion of the composite.

DSC for **GSS$_x$** materials

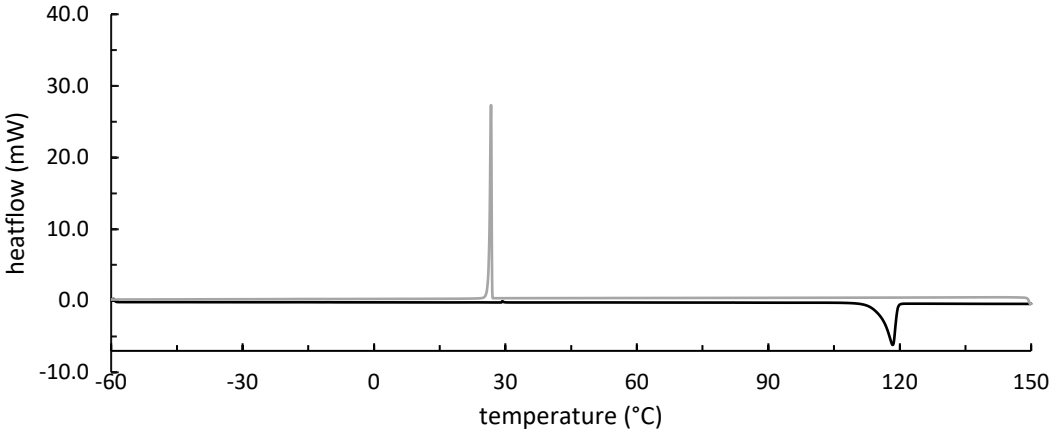


**Figure S8.** DSC heating (black) and cooling (gray) curves from the third cycle for **GSS$_{95}$** exhibiting a melt peak for $S_8$(β) at 118 °C and a crystallization peak at 27 °C.

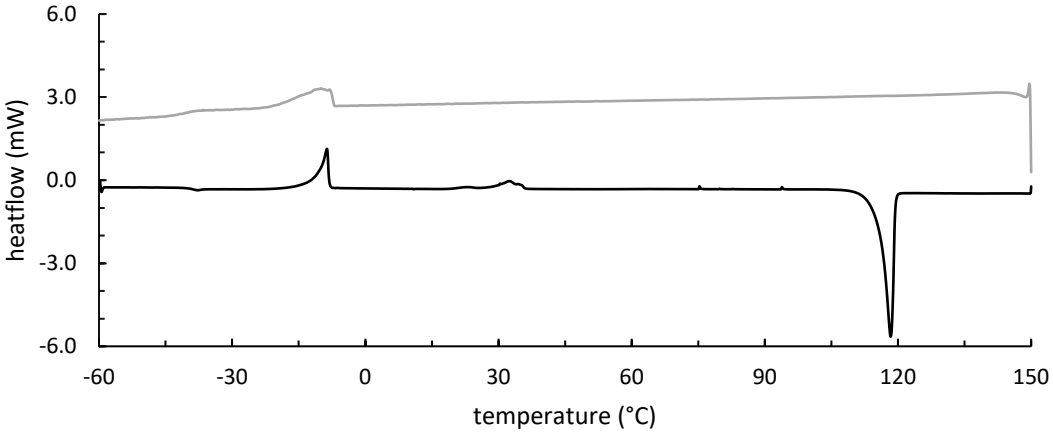


**Figure S9.** DSC heating (black) and cooling (gray) curves from the third cycle for **GSS$_{90}$.** The intensity of the cooling cycle has been multiplied by 4 and shifted by +1.2 mW to make the features appear more prominent. The heating cycle shows a $T_g$ for polymeric sulfur with a midpoint at −39 °C. Two regions of cold crystallization are visible at −24 to −1 °C and from 18 to 39 °C. As in **GSS$_{95}$**, the melt for $S_8$(β) appears at 118 °C. In the cooling cycle, a crystallization exotherm occurs at −12 °C and the reversible $T_g$ is apparent with midpoint at −41 °C.

**Table S3.** $CS_2$ extraction data for **$GSS_x$** and **$OSS_x$** materials

| material | sulfur in composite (wt%)[a] | $CS_2$ soluble (%) | $CS_2$ insoluble (%) | sulfur rank[b] |
|---|---|---|---|---|
| **$GSS_{95}$** | 92.4 | 87.4 | 12.6 | 63 |
| **$GSS_{90}$** | 88.1 | 87.5 | 12.5 | 4 |
| **$OSS_{95}$** | 94.8 | 85.8 | 14.2 | 340 |
| **$OSS_{90}$** | 89.4 | 82.0 | 18.0 | 140 |

[a] Assessed by elemental analysis. [b] The average number of sulfur atoms per crosslink in the material.

$$\text{Sulfur Rank} = \frac{\left\{\frac{\boldsymbol{S_{cov}}}{\boldsymbol{O_{olefin}}}\right\}}{\mathbf{2}} = \left\{\frac{\frac{m_{ins}-m_{org}}{32.06}}{\frac{m_{org}}{mol_{olefin}}}\right\} \qquad \text{(Equation S2)}$$

Data from extraction by $CS_2$ allowed for the calculation of the number of moles of sulfur atoms covalently incorporated ($S_{cov}$) into the materials by subtracting the amount of organic material ($m_{org}$, % organic in the composite · recovered total mass) from the total mass of the insoluble fraction ($m_{ins}$) and dividing by the atomic mass of sulfur (32.06 amu).

The number of olefins in the insoluble fraction was calculated differently depending on the organic material. In both cases, the amount of organic material ($m_{org}$) was divided by the moles of olefin present in 1 mole of monomer. For **$OSS_x$** materials, this number equated to the molecular weight of **OS** multiplied by the percentage of monomers that were modified (as determined by titration). For **$GSS_x$** materials the moles of olefin/ moles of monomer ratio was assessed by determining the weight fraction of monomers and the number of double bonds they contained. An average monomer molecular weight of 169.65 g·mol$^{-1}$ was calculated with 56 mmol of olefin per mol of monomer.

FTIR data of $CS_2$ insoluble fractions of **GSSx** materials

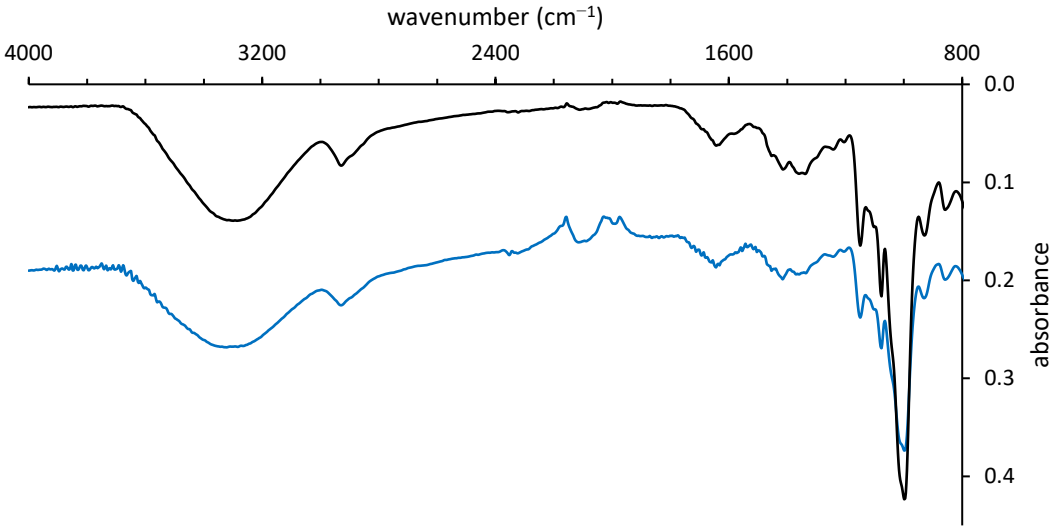


**Figure S10.** FTIR spectra of the $CS_2$ insoluble fractions of **GSS$_{90}$** (black) and **GSS$_{95}$** (blue). The data is presented as collected with increased background absorbance in **GSS$_{95}$** arising from sulfur induced scattering. The stretch at 2080 $cm^{-1}$, indicative of sulfur is also, unsurprisingly, more pronounced. The organic signal (relative to noise) for **GSS$_{90}$** is also stronger than the signal observed for **GSS$_{95}$**.

14. SEM and EDS data for **GSSx** materials

A)

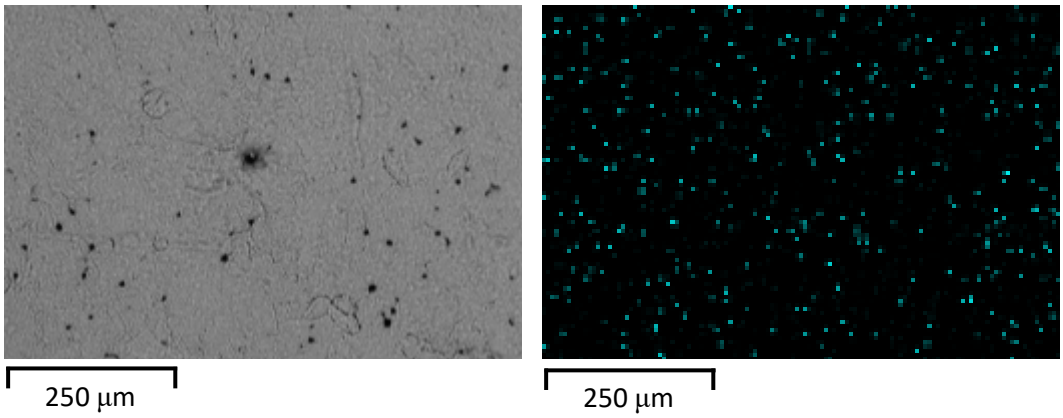


B)

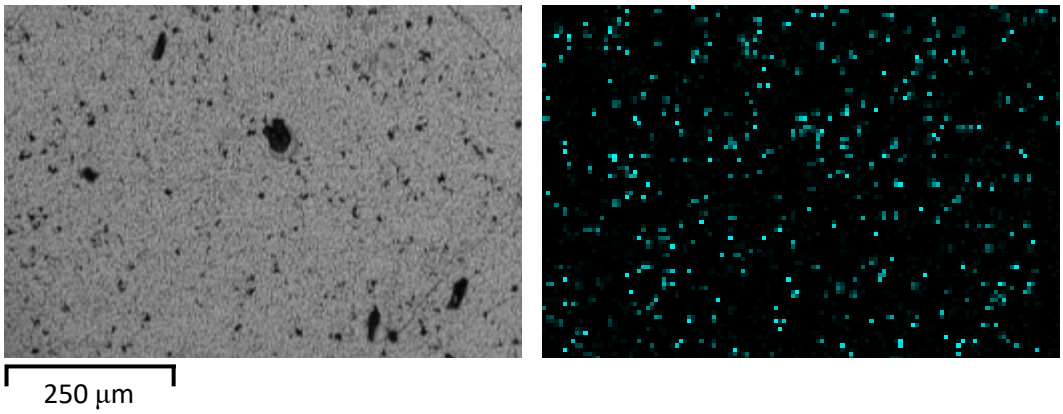


**Figure S11.** SEM images (left) and carbon EDS images (right) of **$GSS_{95}$** (A) and **$GSS_{90}$** (B). Although both materials are in the same morphological regime, the density of organic domains as well as the size of organic domains is obviously larger in **$GSS_{90}$**.

References

1. M. K. Lauer, A. G. Tennyson and R. C. Smith, *Mater. Adv.*, 2021, **2**, 2391-2397.
2. M. K. Lauer, A. G. Tennyson and R. C. Smith, *ACS Appl. Polym. Mater.*, 2020, **2**, 3761-3765.
3. B. Lamy, D. R. Serrano, P. O'Connell, W. Couet, S. Marchand, A.-M. Healy and F. Tewes, *European Journal of Pharmaceutical Research*, 2019, **1**, 2-11.